

Radio-Frequency Plasma Polymers Containing Ionic Phosphonate Groups. 1. Copolymerization of Perfluoroallylphosphonic Acid and Chlorotrifluoroethylene

Michael J. Danilich,[†] Dominic Gervasio,^{‡,1} Donald J. Burton,[§] and Roger E. Marchant^{*||}

Departments of Macromolecular Science, Materials Science, and Biomedical Engineering, Case Western Reserve University, Cleveland, Ohio 44106, and Department of Chemistry, University of Iowa, Iowa City, Iowa 52240

Received October 3, 1994; Revised Manuscript Received April 6, 1995[⊗]

ABSTRACT: Radio-frequency plasma polymer and copolymer films, ranging in thickness from 9 to 660 nm, were prepared from perfluoroallylphosphonic acid (PAPA) and chlorotrifluoroethylene (CTFE). ac conductance measurements showed that the apparent conductivity of the films increased from 1.7 to 4.2 mS/cm as the PAPA content of the comonomer feed was increased from 0 to 100%. Cyclic voltammetry in the presence of chloride indicated that the films were anionic and showed that they were strongly adherent to gold electrodes in aqueous media. As the PAPA content of the comonomer feed was increased, the advancing water contact angle of the films decreased from 98.4° to 8.3° and the solid surface tension (γ_s) of the films increased from 25.4 to 72.5 dyn/cm. High-resolution ESCA and FTIR spectroscopies indicated that increasing the PAPA content of the comonomer feed caused a change in the polymer structure from a highly fluorinated, lightly cross-linked Teflon-like structure to a lightly fluorinated, highly cross-linked structure containing phosphonic acid groups. A mechanism for the formation of the ionic polymer films is proposed in which retention of the phosphonic acid moiety occurs via cleavage of PAPA into fluorocarbon and phosphonate fragments followed by reincorporation of the phosphonic acid into the growing plasma polymer film.

Introduction

Ion-containing polymers, such as ion-exchange resins, polyelectrolytes, and ionomers, are an important class of materials which have found use in many areas.² Ionomers, which contain up to 15 mol % of repeat units with ionic groups in their side chains, have experienced significant growth in the past 30 years. This growth has been driven by the use of perfluorinated ionomers in chlor-alkali production.³ Commercially, the most important of the perfluorinated ionomers is Nafion, a perfluoroalkylsulfonated cation-exchange resin produced by E. I. du Pont de Nemours and Co. Nafion and Nafion-like ionomers have undergone extensive study for fuel cell applications.⁴ Additionally, polymers with bulk as well as surface-grafted sulfonate moieties have been investigated as potential antithrombogenic biomaterials⁵⁻⁸ and as membranes for biomedical sensors.⁹

Although perfluorinated ionomers have excellent chemical and thermal stability, the increasing need for ionic membranes for a range of specialized applications presents challenges that remain unresolved. For example, Nafion films which have been solution cast onto smooth electrode surfaces generally show poor adhesion¹⁰ and mechanical properties.¹¹ Additionally, Nafion 117 exhibits a microbiphasic structure consisting of clusters and channels of sulfonic acid groups interspersed in a hydrophobic fluorocarbon domain.¹²⁻¹⁴ As a result, there is a compromise between the conductance and the permselectivity of such membranes when used in aqueous solution. Increasing the conductance of an ionomer membrane by increasing the relative amount

of sulfonate versus fluorocarbon moieties causes the formation of larger ion channels. The physical dimensions of the ionic channels in Nafion 117 are large enough to permit free migration of ions through the membrane^{11,14,15} and transport of interferent molecules such as small plasma proteins, urea, or ascorbic acid from biological sera.

Novel membrane formulations and processing techniques are being sought to address these problems. Recently, a "Nafion-like" membrane was prepared by plasma copolymerization of trifluoromethanesulfonic acid and chlorotrifluoroethylene.¹⁶ The resulting films were reported to be highly conductive, adherent to a gold electrode substrate, uniform in thickness of less than 1 μm , and pinhole free. Although not reported, it is expected that the high crosslink density typical of plasma polymers¹⁷ hindered the formation of a microbiphasic structure, thus providing enhanced permselectivity.

In this study, the preparation of a series of novel ionic polymers by plasma copolymerization of perfluoroallylphosphonic acid and chlorotrifluoroethylene is reported. Ionic films with phosphonic acid fixed charge groups are expected to possess buffer capacity and enhanced proton conductivity relative to films containing sulfonic acid groups, because of the dibasic nature of the phosphonic acid group. Plasma polymerization of phosphonic acid-containing monomers is an attractive technique for providing novel, highly crosslinked, strongly adherent, thin, ionic membrane materials for a variety of applications where ionic conductance, permselectivity, and biocompatibility are important. Such membranes would be particularly attractive for use with electrochemical biosensors.

Experimental Section

Materials. Chlorotrifluoroethylene (CTFE) ($\text{F}_2\text{C}=\text{CFCl}$, 99+%, inhibited with 1% tributylamine, Aldrich Chemical Co., Inc.), perfluoroallylphosphonic acid (PAPA) ($\text{F}_2\text{C}=\text{CFCF}_2\text{P}(\text{O})-$

* Author to whom correspondence should be addressed.

[†] Department of Macromolecular Science, Case Western Reserve University.

[‡] Department of Materials Science, Case Western Reserve University.

[§] Department of Biomedical Engineering, Case Western Reserve University.

^{||} Department of Chemistry, University of Iowa.

[⊗] Abstract published in *Advance ACS Abstracts*, May 15, 1995.

(OH)₂, methylene iodide (diiodomethane, 99%; Aldrich), perchloric acid (HClO₄; Baker ultrex), ferrous perchlorate (Fe(ClO₄)₂, 99.99%; Johnson-Matthey), ferric perchlorate (Fe(ClO₄)₃, 99.99%; Johnson-Matthey), and reagent-grade sulfuric acid, acetone, methanol, and 100% ethanol were used as received. The preparation and characterization of PAPA have been described elsewhere.¹⁸ PAPA was stored at approximately -5 °C under argon. Distilled, deionized water (DD water) was deionized using a Bantam demineralizer (Barnstead Still and Sterilizer Co.) with a Barnstead standard high-capacity deionizing cartridge (Fisher Scientific Co.) and distilled using a Mega-Pure water still (Corning Glass Works). Aqueous 0.1 M HClO₄/5 mM Fe(ClO₄)₃/5 mM Fe(ClO₄)₂ was prepared as a stock solution using water prepared by reverse osmosis and distillation under N₂.

All glassware was immersed overnight in a sulfuric acid (H₂SO₄)/Nochromix (Godax Laboratories, Inc.) solution, washed with a Liquinox (Alconox, Inc.) soap solution, rinsed with tap water, DD water, and methanol, and dried at 100 °C.

Substrates. The substrates used as supports for the plasma polymers included clean glass microslides, gold-coated silicon wafers, germanium internal reflection elements, and gold interdigitated electrodes. Glass microslides (25 × 75 mm) were immersed in sulfuric acid overnight, thoroughly rinsed with tap water, DD water, and acetone, then washed with refluxing acetone in a Soxhlet extraction system for at least 24 h, rinsed with DD water and 100% ethanol, and dried overnight at 80–100 °C. Silicon wafers (111 face, 2 in. diameter, n-type, resistivity 3.5–6.6 ohms; Wacker, Inc.) were cleaned using standard clean and degrease procedures.¹⁹ The silicon substrate was heated to 110 °C, and approximately 5 nm of chromium was deposited followed by approximately 200 nm of gold using a CVC 409 thermal evaporation system. The gold-coated wafers were then scored on the uncoated silicon surface into 1 × 2 cm rectangles using a diamond saw.

Gold interdigitated electrodes with 100- μ m-wide electrode lines separated by 50 μ m were deposited onto alumina substrates using conventional photolithography methods. Individual 5 × 6 mm electrodes were cut from alumina using the diamond saw. The electrodes were cleaned electrochemically by cycling in 0.05 M aqueous sulfuric acid at 100 mV/s between -0.3 and +1.6 V versus a saturated calomel reference electrode (SCE) using a gold counter electrode. Cycling of the electrodes was carried out for approximately 5 min until no residual contaminant peaks were observed in the gold voltammogram. A cell constant for the electrodes was determined from conductance measured in 1 M aqueous KCl solution.

Plasma Deposition System and Procedure. The plasma deposition system was identical to the system used in previous studies²⁰ with the exception of a modification to the radio-frequency (RF) power coupling system. The RF coupling system used in this study consisted of two individual 12.5-mm-wide copper strips. This coupling system provided a uniform, intense glow throughout the reactor with the monomers and conditions used in this study.

Substrates were mounted on clean glass slides suspended on a glass rod tray. PAPA was placed in a round-bottomed flask and heated to approximately 90 °C. The flask was coupled to its inlet line via a glass stopcock (Ace Glass Inc.) fitted with a Teflon plunger and Viton O-rings. The glass PAPA inlet to the reaction chamber extended 14.5 cm beyond the upstream end of the reactor head. The CTFE source was a small cylinder of pressurized CTFE fitted with a pressure regulator and a series of Nupro metering valves. CTFE was introduced into the reactor through an inlet which terminated at the upstream end of the reactor head. The reactor was evacuated for at least 1 h, and the system was examined for leaks.¹⁹ PAPA was degassed by four or five freeze-thaw cycles under vacuum using liquid nitrogen and a heating mantle.

An initial argon plasma treatment (30 mTorr, 40 W net discharge power, 1.9 cm³(STP)/min argon flow rate) was carried out for 5 min prior to each plasma polymerization reaction. After the argon discharge, the argon flow was stopped, the system was evacuated, and CTFE and PAPA were introduced into the reaction chamber. Steady-state monomer flow rates were calculated from the measured rise in pressure

Table 1. PAPA/CTFE Plasma Polymerization Conditions^a

material	preplasma CTFE flow rate (cm ³ (STP)/min)	preplasma PAPA flow rate (cm ³ (STP)/min)	duration (min)
PPCTFE	5.4	0	60
PPCTFE	4.8	0	80
PPCTFE	1.9	0	120
30% PAPA	0.32	0.14	120
70% PAPA	0.046	0.13	120
PPPAPA	0	0.04	120
PPPAPA	0	0.10	120
PPPAPA	0	0.19	60

^a Net discharge power, 40 W; discharge pressure, 30 mTorr; CTFE, chlorotrifluoroethylene; PAPA, perfluoroallylphosphonic acid; PPCTFE, plasma-polymerized chlorotrifluoroethylene; 30% PAPA, 30:70 plasma copolymer of perfluoroallylphosphonic acid:chlorotrifluoroethylene; 70% PAPA, 70:30 plasma copolymer of perfluoroallylphosphonic acid:chlorotrifluoroethylene; PPPAPA, plasma-polymerized perfluoroallylphosphonic acid.

(with time) in the reaction chamber with the vacuum shutoff valve closed.¹⁷ A series of plasma copolymers were prepared at 30 mTorr and 40 W (net) for 60, 80, or 120 min. The plasma copolymers were distinguished by the percent of PAPA in the comonomer feed, determined from the preplasma monomer flow rates (Table 1). After the discharge was extinguished, the reactor pressure was maintained at 30 mTorr for 5 min. Monomer flow was stopped, and the reactor was evacuated overnight. The reactor was raised to atmospheric pressure with argon, and the samples were removed from the reactor and stored in a desiccator.

Characterization Methods. Physical Methods. The thicknesses of the plasma-polymerized films deposited onto gold-coated silicon wafers were calculated from ellipsometry data using a Fortran program.²¹ Measurements were made with a Gaertner L117 production ellipsometer with a helium/neon source under "cleanroom" conditions. Three measurements were made on each sample. To carry out the thickness calculations, the index of refraction of the plasma polymer films was assumed to be 1.54, the mean index of refraction of a number of plasma polymers prepared in the reaction system used in this study.^{20,22–24} Errors in thickness due to deviation of the index of refraction of individual plasma polymers from 1.54 are expected to be less than 10%.

Advancing (θ_A) and receding (θ_R) distilled water and methylene iodide contact angles on plasma-polymerized films deposited onto glass microslides were measured in air (22.8 ± 1.4 °C, 40.0 ± 5.3% relative humidity) by the sessile drop method²⁵ using a Rame-Hart contact angle goniometer (Model 100-00). Contact angle measurements were generally carried out within 2 days of sample preparation. Contact angle measurements were repeated five times, after the initial drop was placed on the polymer surface and after each of four successive additions (approximately 2 μ L each) to the initial drop. This represented measurement of θ_A for one spot on the sample. θ_R was obtained by measuring the contact angle after each of successive 2 μ L aliquot withdrawals from the remaining drop at the same spot. Measurements were repeated at four or five different spots on each sample. θ_A and θ_R for each sample were the calculated means of the advancing and receding angles at each spot. Solid surface tensions were calculated from these data using the method of Kaelble.²⁶

Spectroscopic Methods. Electron spectroscopy for chemical analysis (ESCA) was carried out on plasma polymer films deposited onto gold-coated silicon wafers using a Perkin-Elmer PHI 5400 X-ray photoelectron spectrometer. The incident radiation consisted of Mg K α X-rays, and the take-off angle was fixed at 45°. For survey spectra, the 0–1100-eV binding energy region was analyzed at 50 ms/step and 0.5 eV/step. The analyzer pass energy was set at 178.95 eV. For high-resolution studies, a 20-eV binding energy window was analyzed in the region of interest at 50 ms/step and 0.1 eV/step. The analyzer pass energy was set at 35.75 eV. High-resolution spectra were deconvoluted into constituent Gaussian-Lorentzian peaks

using a peak-fitting program. The constituent peaks were initially 80% Gaussian and 1.7-eV full width at half-maximum (fwhm). A maximum of 25 iterations was carried out until convergence was attained with no additional constraints on the constituent peaks.

Attenuated total reflectance Fourier transform infrared (ATR-FTIR) spectra of plasma polymer films deposited onto $50 \times 20 \times 2$ mm trapezoidal germanium internal reflection elements were obtained using a Digilab FTS-40 FTIR spectrometer equipped with an attenuated total reflectance (ATR) optical accessory (Wilkes Scientific, Model 50) and a magnesium-cadmium-telluride (MCT) detector. Germanium crystals were cleaned by polishing with alumina (Buehler gamma micro polish II, 0.05 μm particle size) on a velour pad and rinsing with water, DD water, and 100% ethanol. ATR-FTIR spectra with a resolution of 8 cm^{-1} were obtained by averaging 2048 sample and reference scans. Transmission FTIR spectra of PAPA (monomer) spread onto a KBr window were obtained with the FTS-40 and a triglycine sulfate (TGS) detector. Transmission spectra with a resolution of 8 cm^{-1} were obtained by averaging 1024 sample and reference scans.

Electrochemical Methods. Plasma-polymerized films approximately 500 nm thick were deposited directly onto interdigitated electrodes for electrochemical studies. Aluminum foil masks were used to keep the electrode bonding pads free of plasma polymer deposits. The aluminum foil was cleaned by sonication in ethanol for at least 15 min and air dried.

The conductivity of films deposited onto interdigitated electrodes was estimated using an ac conductance technique. The coated electrode array was connected to an ac impedance bridge (Beckman Model RC-19 conductivity bridge) using alligator clips. The coated portion of the interdigit array was immersed in DD water ($18 \text{ M}\Omega\cdot\text{cm}$), and the resistance was measured. Capacitive effects were eliminated using external capacitors. Effects of the leads between the interdigits and the bonding pads were considered to be negligible.

Cyclic voltammetry was used to characterize the electrochemical processes occurring on coated and uncoated electrodes. Experiments were carried out by placing the coated or uncoated interdigitated (working) electrode and a gold counter electrode in a standard two-compartment glass electrochemical cell filled with 0.1 M HClO_4 /5 mM $\text{Fe}(\text{ClO}_4)_3$ /5 mM $\text{Fe}(\text{ClO}_4)_2$. The external SCE reference was connected to the bulk solution via a salt bridge filled with the supporting solution. For experiments carried out in the presence of chloride, a saturated aqueous solution of KCl was injected into the cell using a syringe until the chloride concentration was 0.1 M. The potential of the gold working electrode was cycled linearly at 100 mV/s between -0.1 and $+0.8$ V vs SCE. The resulting current between the working and counter electrodes was measured. Potential scans were initiated in the positive (anodic) sweep direction.

Results

Ellipsometry. The thicknesses of the plasma polymer films, calculated from ellipsometry data, were between 9 and 660 nm. Plasma polymer deposition rates, calculated by dividing the film thickness by the duration of the deposition reaction, ranged from 5 to 70 $\text{\AA}/\text{min}$. These were considerably lower than the deposition rates obtained for other plasma polymers prepared in the same system.²⁴ PPCTFE exhibited a steep decrease in deposition rate with downstream distance in the plasma reactor, decreasing from 60 $\text{\AA}/\text{min}$ at the front of the reactor to 5 $\text{\AA}/\text{min}$ 215 mm downstream. 30% PAPA, 70% PAPA, and PPPAPA deposited relatively uniformly, decreasing in thickness only slightly with downstream distance in the reactor. The mean deposition rates of these plasma polymers were 28.1 ± 5.2 (30% PAPA), 38.4 ± 14.8 (70% min), and 41.7 ± 10.5 $\text{\AA}/\text{min}$ (PPPAPA). The deposition rates of PPPAPA and PPCTFE were independent of monomer flow rate for the small range of flow rates used in this

Table 2. Plasma-Copolymerized PAPA/CTFE Contact Angles and Solid Surface Tension^a

material	$\theta_A(\text{H}_2\text{O})$ (deg)	$\theta_A(\text{CH}_2\text{I}_2)$ (deg)	γ_s (dyn/cm)	γ_s^p (dyn/cm)	γ_s^d (dyn/cm)
PPCTFE	98.4 ± 1.2	65.5 ± 0.9	25.4	1.3	24.1
30% PAPA	80.8	61.7	30.5	7.8	22.7
70% PAPA	41.6				
PPPAPA	8.3 ± 3.9	55.4 ± 6.0	72.5	55.7	16.8

^a Values are means \pm standard errors. PPCTFE, plasma-polymerized chlorotrifluoroethylene; 30% PAPA, 30:70 plasma copolymer of perfluoroallylphosphonic acid:chlorotrifluoroethylene; 70% PAPA, 70:30 plasma copolymer of perfluoroallylphosphonic acid:chlorotrifluoroethylene; PPPAPA, plasma-polymerized perfluoroallylphosphonic acid. θ_A , advancing contact angle; θ_R , receding contact angle; H_2O , water probe; CH_2I_2 , methylene iodide probe; γ_s , solid surface tension; γ_s^p , polar component of the solid surface tension; γ_s^d , dispersive component of the solid surface tension.

study. Similarly, the composition and properties of the three PPCTFEs and PPPAPAs, determined from contact angle measurements, ESCA, and ATR-FTIR, were found to be independent of monomer flow rate and film thickness. Accordingly, contact angle and spectroscopic results obtained from the three PPCTFEs and the three PPPAPAs are presented and discussed together.

Contact Angles. Water and methylene iodide contact angles decreased with increasing PAPA content in the comonomer feed (Table 2). The water contact angle was especially sensitive, decreasing approximately linearly from 98.4° for PPCTFE to less than 9.0° for PPPAPA. The solid surface tension increased with increases in PAPA in the comonomer feed from 25.4 dyn/cm for PPCTFE to 72.5 dyn/cm for PPPAPA (Table 2). This was reflective of a large increase in the polar component of the solid surface tension from 1.3 to 55.7 dyn/cm and a slight, concurrent decrease in the dispersive component of the solid surface tension from 24.1 to 16.8 dyn/cm.

ESCA. The atomic compositions of the plasma polymer surfaces, determined from ESCA survey spectra,^{27,28} are compiled in Table 3. The fluorine, chlorine, phosphorus, and oxygen compositions qualitatively followed trends expected from the monomer structures, with the fluorine and chlorine contents decreasing and the phosphorus and oxygen contents increasing with increasing PAPA in the comonomer feed. Quantitatively, however, the chlorine and fluorine contents of the films were generally lower than expected, whereas the oxygen content of the films was generally higher than expected. Conversely, the carbon content, which was expected to decrease with increases in PAPA in the comonomer feed, remained constant. The phosphorus content of the films was equivalent, within experimental error, to its theoretical value. Some nitrogen also was incorporated into the films, especially those which contained PAPA in the comonomer feed.

High-resolution C 1s spectra of plasma polymers are presented in Figure 1. The spectra have not been shifted to account for sample charging during scanning. In general, the C 1s spectra of the PAPA-containing plasma polymers (Figure 1B,C) were narrow and were shifted to low binding energies compared with the C 1s spectrum of PPCTFE (Figure 1A). The results of C 1s spectral deconvolutions are shown in Table 4. The assignments of the C 1s constituent peaks for PPCTFE are consistent with ESCA studies of Kel-F²⁹ and polypropylene treated with a CTFE discharge under nonpolymerizing conditions.³⁰ The assignment of C-P at 286.2 eV is speculative. The constituent peaks attributed to

Table 3. Plasma-Copolymerized PAPA/CTFE Atomic Percent Composition^a

material	C 1s	F 1s	O 1s	P 2p	Cl 2p	N 1s	other
CTFE ^b	33.3	50.0	0.0	0.0	16.7	0.0	0.0
PPCTFE	36.7 ± 2.1	52.8 ± 1.0	2.1 ± 2.8	0.0 ± 0.0	7.8 ± 1.9	0.6 ± 0.8	0.0 ± 0.0
30% PAPA	38.5 ± 2.8	42.3 ± 4.2	5.7 ± 6.1	0.4 ± 0.5	8.3 ± 4.9	4.8 ± 0.3	0.0 ± 0.0
70% PAPA	34.8	37.0	17.0	4.0	0.5	3.2	3.4
PPPAPA	36.9 ± 8.8	14.1 ± 4.1	34.1 ± 7.6	8.4 ± 2.9	0.1 ± 0.1	6.2 ± 2.4	0.3 ± 0.6
PAPA ^b	25.0	41.7	25.0	8.3	0.0	0.0	0.0

^a Values are means ± standard deviations. CTFE, chlorotrifluoroethylene; PAPA, perfluoroallylphosphonic acid; PPCTFE, plasma-polymerized chlorotrifluoroethylene; 30% PAPA, 30:70 plasma copolymer of perfluoroallylphosphonic acid:chlorotrifluoroethylene; 70% PAPA, 70:30 plasma copolymer of perfluoroallylphosphonic acid:chlorotrifluoroethylene; PPPAPA, plasma-polymerized perfluoroallylphosphonic acid. ^b Theoretical values.

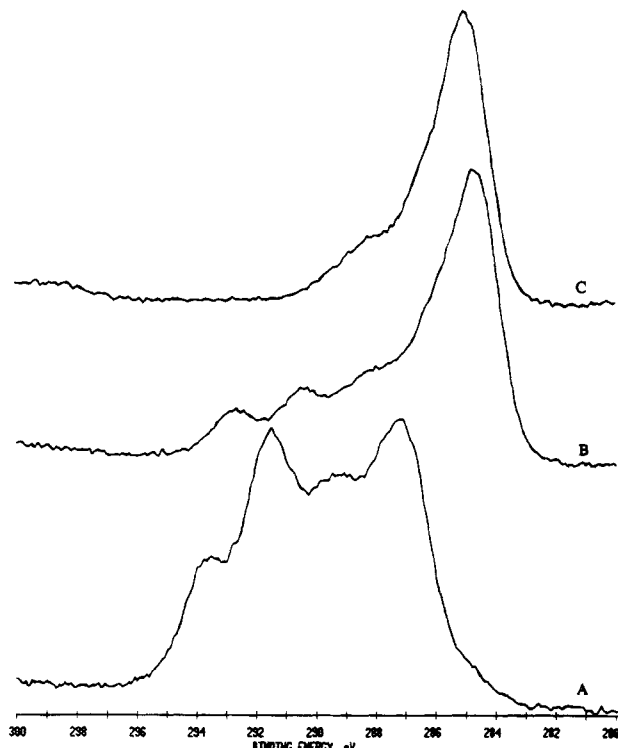


Figure 1. High-resolution C 1s ESCA Spectra. (A) PPCTFE: plasma-polymerized chlorotrifluoroethylene. (B) 70% PAPA: 70:30 plasma copolymer of perfluoroallylphosphonic acid:chlorotrifluoroethylene. (C) PPPAPA: plasma-polymerized perfluoroallylphosphonic acid.

Table 4. Plasma-Copolymerized PAPA/CTFE Deconvoluted C 1s Peak Areas and Assignments^a

position (eV)	assignment	% C 1s peak area		
		PPCTFE	70% PAPA	PPPAPA
284.8	quaternary carbon	<i>b</i>	42.0	51.3
285.0	hydrocarbon	5.3	<i>b</i>	<i>b</i>
286.2	C-P, C-O	<i>b</i>	19.8	28.3
287.2	quaternary carbon, CCl	26.8	<i>b</i>	<i>b</i>
287.7	CF, C=O	<i>b</i>	<i>b</i>	9.3
288.4	CF	<i>b</i>	17.2	4.6
289.5	CF, CFCl	29.8	<i>b</i>	4.5
290.6	CF ₂	<i>b</i>	13.4	<i>b</i>
291.7	CF ₂	26.0	<i>b</i>	<i>b</i>
292.5	CF ₃	<i>b</i>	<i>b</i>	2.0
292.9	CF ₃	<i>b</i>	7.6	<i>b</i>
293.8	CF ₃	12.0	<i>b</i>	<i>b</i>

^a PPCTFE, plasma-polymerized chlorotrifluoroethylene; 70% PAPA, 70:30 plasma copolymer of perfluoroallylphosphonic acid:chlorotrifluoroethylene; PPPAPA, plasma-polymerized perfluoroallylphosphonic acid. ^b Peak absent.

CF₃, CF₂, and CF shifted 1.3–1.8 eV negative as the PAPA content of the comonomer feed was increased from 0% to 100%.

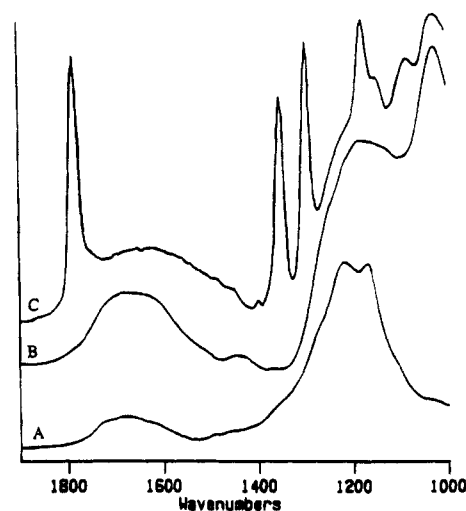


Figure 2. FTIR Spectra. (A) ATR spectrum of PPCTFE (plasma-polymerized chlorotrifluoroethylene). (B) ATR spectrum of PPPAPA (plasma-polymerized perfluoroallylphosphonic acid). (C) Transmission spectrum of PAPA (perfluoroallylphosphonic acid).

F 1s, O 1s, Cl 2p, and P 2p high-resolution ESCA spectra of the four plasma polymers were generally quite broad and were deconvoluted into two or three constituent peaks. The maximum intensity of the F 1s spectra shifted position from approximately 689.4 to 687.5 eV as the PAPA content of the comonomer feed was increased from 0% to 100%. Similarly, the Cl 2p peak shifted from 202.4 to 200.8 eV over the comonomer composition range of 0% PAPA to 70% PAPA. The O 1s high-resolution peak decreased in width and shifted slightly from 532.8 to 532.4 eV, and the P 2p peak shifted from 136.0 to 134.6 eV but broadened slightly as the PAPA content of the comonomer feed increased from 30% to 100%.

FTIR. FTIR spectra of PAPA, PPPAPA, and PPCTFE are presented in Figure 2. Band assignments are provided in Table 5. The FTIR spectrum of PPCTFE (Figure 2A) exhibited a broad, weak absorption between 1750 and 1550 cm⁻¹ and strong absorptions centered at approximately 1220 and 1177 cm⁻¹. The broad band between 1750 and 1550 cm⁻¹ is attributed to a variety of C=O stretching absorptions.^{31,32} The absorptions at 1220 and 1177 cm⁻¹ are attributed to C-F stretching absorptions in a variety of fluorocarbon moieties (CF, CF₂, CF₃).³³⁻³⁵ The ν(C=O) band was broadened and intensified in FTIR spectra of PPPAPA (Figure 2B). This is attributed to an overlapping O-H deformation absorption associated with P(O)(OH)₂.³⁵⁻³⁷ Additionally, in the spectra of PPPAPA, the ν(C-F) absorptions appeared to have merged into a single broad peak and a new absorption band, attributed to P-O stretching in P-OH,^{35,37} appeared at 1018 cm⁻¹.

Table 5. Plasma-Copolymerized PAPA/CTFE Infrared Band Assignments^a

assignment	position (cm ⁻¹)		
	PPCTFE	PPPAPA	PAPA
$\nu(\text{C}=\text{C})$	<i>b</i>	<i>b</i>	1786
$\delta(\text{O}-\text{H})$ in $\text{P}(\text{O})(\text{OH})_2$	<i>b</i>		1700–1425
+	<i>b</i>	1700–1425	
$\nu(\text{C}=\text{O})$	1750–1550		<i>b</i>
$\nu_a(\text{C}-\text{F})$ in $\text{CF}_2=$	<i>b</i>	<i>b</i>	1350
$\nu_s(\text{C}-\text{F})$ in $\text{CF}_2=$	<i>b</i>	<i>b</i>	1296
$\nu(\text{C}-\text{F}) + \nu(\text{P}=\text{O})$	<i>b</i>	1230–1170	1215 (shoulder)
$\nu(\text{C}-\text{F})$	1220, 1177	<i>b</i>	<i>b</i>
$\nu(\text{C}-\text{F})$ in $\text{CF}=\text{}$	<i>b</i>	<i>b</i>	1176
$\nu_s(\text{C}-\text{F})$ in $\text{CF}_2=$	<i>b</i>	<i>b</i>	1084
$\nu(\text{P}-\text{O})$ in POH	<i>b</i>	1018	1018

^a PPCTFE, plasma-polymerized chlorotrifluoroethylene; PPPAPA, plasma-polymerized perfluoroallylphosphonic acid; PAPA, perfluoroallylphosphonic acid; ν , stretching vibration; δ , bending vibration; a, asymmetric mode; s, symmetric mode. *b* Peak absent.

Table 6. Plasma-Copolymerized PAPA/CTFE $\nu(\text{P}-\text{O})/\nu(\text{C}-\text{F})$ Infrared Absorbance Band Ratio^a

material	$\nu(\text{P}-\text{O})/\nu(\text{C}-\text{F})$
PPCTFE	0.10
30% PAPA	0.32
70% PAPA	0.45
PPPAPA	1.4

^a PPCTFE, plasma-polymerized chlorotrifluoroethylene; 30% PAPA, 30:70 plasma copolymer of perfluoroallylphosphonic acid; chlorotrifluoroethylene; 70% PAPA, 70:30 plasma copolymer of perfluoroallylphosphonic acid; chlorotrifluoroethylene; PPPAPA, plasma-polymerized perfluoroallylphosphonic acid.

A transmission FTIR spectrum of PAPA is included in Figure 2 for comparison with the spectrum of PPPAPA. The FTIR spectrum of PAPA has been discussed in detail elsewhere.³⁷ Strong absorptions at 1786 and 1350 cm⁻¹ and a moderately strong absorption at 1084 cm⁻¹, all associated with the perfluorinated vinyl bond,³⁵ dominate the FTIR spectrum of PAPA (Figure 2C). The absence of these bands in the FTIR spectrum of PPPAPA indicates that the vinyl bond in PAPA participated in the plasma polymerization reaction. A sharp band at 1296 cm⁻¹ is attributed to asymmetric C–F stretching in CF₂. This band is absent in the PPPAPA spectrum and is present as a weak shoulder in the PPCTFE spectrum. The presence of a moderately strong shoulder at approximately 1215 cm⁻¹ in the monomer spectrum, attributed to bonded P=O stretching,^{35,37} suggests that the apparent broadening and merging of the $\nu(\text{C}-\text{F})$ absorptions at approximately 1200 cm⁻¹ in the PPPAPA spectrum was the result of a $\nu(\text{P}=\text{O})$ contribution in the same region. The broad absorption between 1700 and 1425 cm⁻¹ in the PPPAPA spectrum attributed to $\delta(\text{O}-\text{H})$ in $\text{P}(\text{O})(\text{OH})_2$ was also observed in the PAPA spectrum. The ATR-FTIR spectra of 30% PAPA and 70% PAPA contain features common to the spectra of PPCTFE and PPPAPA, with the ratio of $\nu(\text{P}-\text{O})$ (1018 cm⁻¹) intensity to $\nu(\text{C}-\text{F})$ (approximately 1200 cm⁻¹) intensity increasing with increases in the PAPA content in the comonomer feed (Table 6). The PPCTFE spectrum is featureless in the region between 4000 and 2000 cm⁻¹, not shown in Figure 2. Two broad absorptions in this region in the spectra of PAPA monomer and PAPA-containing plasma polymers are attributed to $\nu(\text{O}-\text{H})$ in $\text{P}(\text{O})(\text{OH})_2$.^{35–37}

Conductivity. The apparent conductivities of the plasma polymer films are presented in Table 7. The conductivity is defined as “apparent conductivity” because the plasma polymer membranes were too thin to

Table 7. Plasma-Copolymerized PAPA/CTFE Apparent Conductivities^a

material	apparent conductivity (mS cm ⁻¹)
PPCTFE	1.7
30% PAPA	2.3
PPPAPA	4.2

^a Films approximately 500 nm thick. PPCTFE, plasma-polymerized chlorotrifluoroethylene; 30% PAPA, 30:70 plasma copolymer of perfluoroallylphosphonic acid; chlorotrifluoroethylene; PPPAPA, plasma-polymerized perfluoroallylphosphonic acid

fill the entire volume of space encompassed by the alternating electric field determined by the interdigitated cell geometry at 1-kHz ac stimulation.³⁸ The apparent conductivity is considered the weight average of the conductivities of the regions inside and outside the membrane. The contribution from the region outside the membrane was assumed to be constant regardless of the coating on the interdigitated electrode. Accordingly, since the plasma polymer films of different compositions had comparable thicknesses, the data in Table 7 provide a relative measure of the conductivities of the plasma polymer films. The apparent conductivity increased approximately linearly from 1.7 mS/cm for PPCTFE to 4.2 mS/cm for PPPAPA. The conductivity calculated for the bare gold interdigitated electrodes in pure water (3.0 mS/cm) was higher than expected based on the conductivity of the water as determined with a Yellow Springs Instrument Co. (YSI) conductivity probe (5.7 $\mu\text{S}/\text{cm}$). The high conductance of the bare gold electrode was attributed to the wetted alumina in the spaces between the gold electrode lines. The relative conductivities measured with gold electrode arrays coated with PPCTFE or with 30% PAPA were lower than the conductivity measured with an identical but uncoated electrode array because of an inability of water to wet the alumina substrate when the gold array was coated with these hydrophobic membrane materials.

Cyclic Voltammetry. Figure 3 shows the cyclic voltammograms of gold interdigitated electrodes coated with PPCTFE (dashed line) or PPPAPA (solid lines) in an aqueous 0.1 M HClO₄/0.1 M KCl/5 mM Fe(ClO₄)₃/5 mM Fe(ClO₄)₂ solution. The cyclic voltammogram of gold coated with PPPAPA initially showed low Fe²⁺ oxidation (Fe²⁺ → Fe³⁺) current. As potential cycling continued, however, the Fe²⁺ oxidation current increased with each subsequent sweep until a steady state was attained. The initially low Fe²⁺ oxidation current and subsequent increases in oxidation current on cycling were reproduced after the coated electrode was soaked in distilled water and the measurement was repeated. In contrast, an uncoated gold electrode which was soaked in distilled water and readmitted to the cell immediately exhibited high Fe²⁺ oxidation kinetics (solid line trace in Figure 4). The cyclic voltammetry of a gold electrode coated with the PPCTFE (dashed line, Figure 3) exhibited significantly reduced oxidation and reduction currents, suggestive of a partially insulating membrane.

Discussion

This work was motivated by the need, in the areas of biosensors and fuel cells, for ionically conductive, permselective polymer membrane materials which are strongly adherent to smooth inorganic supports in aqueous solution. PAPA was chosen because of the enhanced ionic conductivity and buffering properties expected to result from the dibasic nature of the phosphonic acid

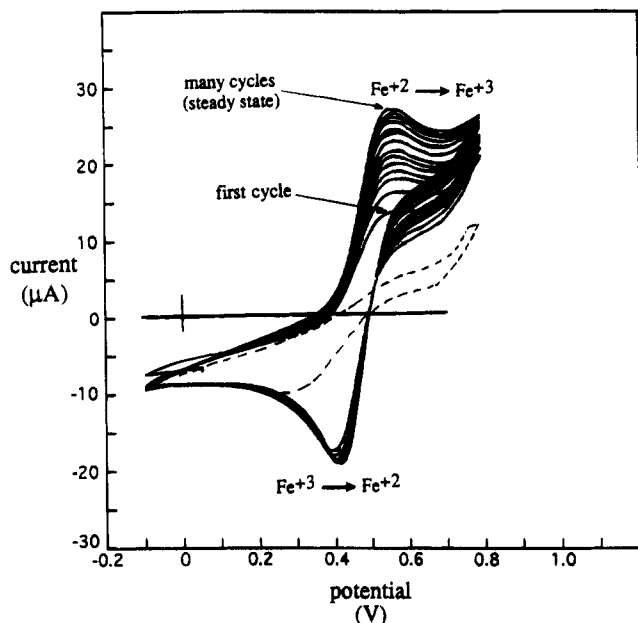


Figure 3. Cyclic voltammograms of coated gold. Solid lines: PPPAPA (plasma-polymerized perfluoroallylphosphonic acid) coating. Dashed line: PPCTFE (plasma-polymerized chlorotrifluoroethylene) coating. Solution: 0.1 M HClO_4 /0.1 M KCl/5 mM $\text{Fe}(\text{ClO}_4)_2$ /5 mM $\text{Fe}(\text{ClO}_4)_3$. Films approximately 500 nm thick. Working electrode area: 4.2 mm². Reference: SCE. Counter: gold. Scan rate: 100 mV/s.

Table 8. Calculated Bond Dissociation Energies in CTFE and PAPA

bond	bond energy (eV)		bond	bond energy (eV)	
	CTFE	PAPA		CTFE	PAPA
C-F (CF ₂ =)	4.6	4.4	C-C	c	3.6
C-F (CFCl)	4.5	c	C-P	c	3.8
C-F (=CF ⁻)	c	4.4	P=O	c	6.7
C-F (-CF ₂ P ⁻)	c	4.3	P-O	c	4.5
C-Cl (CFCl)	3.9	c	O-H	c	4.8
C=C ^b	6.3	6.3			

^a CTFE, chlorotrifluoroethylene; PAPA, perfluoroallylphosphonic acid. ^b Opening of the C=C π bond requires approximately 2.74 eV (from ref 17). ^c Bond not present.

group. Plasma polymerization was employed because the high degree of crosslinking common to plasma polymers was expected to suppress the formation of a microbiphasic structure commonly observed in conventional ionomer membranes and limit ancillary problems such as mechanical fragility and an inverse relationship between permselectivity and ionic conductance.

Composition and Structure. The wide range of water contact angles and solid surface tensions exhibited by the series of CTFE/PAPA plasma polymers (Table 2) showed that the PAPA content of the comonomer feed had a significant influence on the relative concentration of polar functional groups in the plasma polymer films. The strong, approximately linear increase in the polar component of the solid surface tension with increasing PAPA in the comonomer feed is consistent with an increasing concentration of polar functional groups in the plasma polymer series.

The atomic compositions of the plasma polymer films followed the trends expected from stoichiometry and the structures of CTFE and PAPA. Quantitative deviations from these expected trends can be attributed to differences in the specific bond dissociation energies of CTFE and PAPA, presented in Table 8. Dissociation energies for bonds in CTFE and PAPA, calculated on the basis

of the dual covalent/ionic nature of chemical bonds,³⁹ range from 3.6 to 6.7 eV. Dissociation in a radio-frequency glow discharge is typically attributed to collision with an electron.^{17,40} The distribution of electrons in such a discharge contains a significant number of electrons possessing sufficient energy to break any organic bond. The bonds with the highest probability of dissociation following electron impact are expected to be those with the lowest dissociation energy. The weakest bond in CTFE is the C-Cl bond in CTFE. Thus, cleavage of the C-Cl bond in CTFE and subsequent removal of chlorine and chloride from the reactor account for the low chlorine content of the plasma polymers (Table 3). Similarly, 2.74 eV is sufficient to open the C=C π bond in either monomer and generate a free radical.¹⁷ The disappearance of this low-energy conjugated bond after plasma polymerization is clearly evident from comparison of the IR spectra of PAPA and the plasma polymers.

Etching and ablation of fluorine commonly compete with polymer-forming mechanisms in fluorocarbon discharges^{41,42} and probably account for the low deposition rates and the low fluorine contents of the plasma-polymerized films. The loss of fluorine was more pronounced in PAPA-containing films than in PPCTFE because of the reduced relative concentration of easily cleaved C-Cl bonds and the increased residence time of monomers in the glow discharge resulting from the reduced overall monomer flow rate. The increased ablation of fluorine with increased PAPA in the comonomer feed resulted in increased cross-linking, as evidenced by the large tertiary and quaternary carbon contributions to ESCA C 1s spectra. Similarly, the shifts for the C 1s, F 1s, O 1s, Cl 2p, and P 2p ESCA peaks to lower binding energies are consistent with a reduction in the extent of shielding and delocalization of inner-shell electrons as the plasma polymer structure changed from a highly fluorinated, lightly cross-linked Teflon-like structure to a lightly fluorinated, highly cross-linked structure containing polar phosphonate substituents. A similar systematic shift of F 1s peaks and C 1s constituent peaks attributed to CF₃, CF₂, and CF to lower energy was observed in an ESCA study of ethylene and fluoroethylenes.²⁹

Phosphorus was retained by the plasma polymers in stoichiometrically expected amounts (Table 3). Assuming identical electron collision cross-sections for C-C, C-P, and C-F bonds in PAPA, this indicated that phosphonate fragments generated by cleavage of the C-C and C-P linkages were reincorporated into the growing plasma polymer film. Dissociation of the relatively weak O-H bond in reincorporated phosphonic acid was of concern, but the FTIR bands at 1018 and 1750–1450 cm⁻¹ associated with P-OH and P(O)(OH)₂ and the shoulder at 1215 cm⁻¹ associated with P=O strongly suggest that intact phosphonic acid groups were retained by the PAPA-containing plasma polymers.

The incorporation of atmospheric oxygen at trapped free-radical sites is also quite common in plasma polymerization⁴³ and was evident from the composition of PPCTFE, which contained 2.1% oxygen and also in PAPA-containing plasma polymers where the O/P atomic ratio was consistently higher than the PAPA value of 3 (Table 3). FTIR spectra indicated that the majority of the incorporated oxygen was in the form of carbonyl.

Ionic Properties. Ionic conductivity is an essential property of a polymer for electrochemical applications

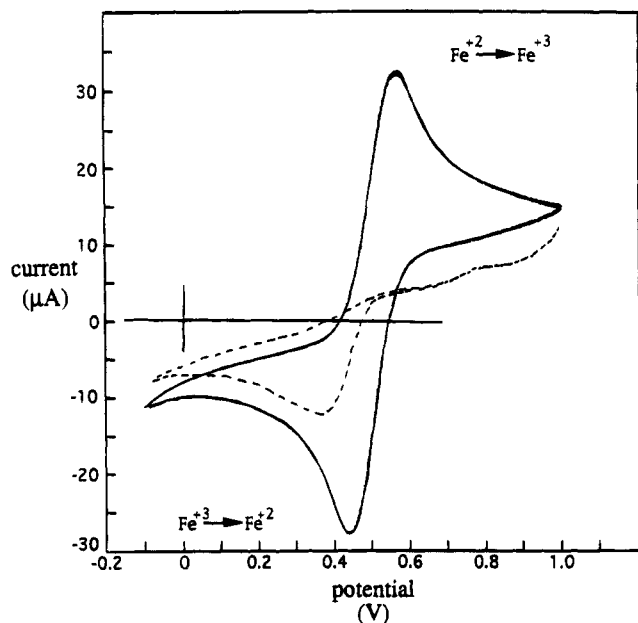


Figure 4. Cyclic voltammograms of uncoated gold. Solid line: 0.1 M KCl in solution. Dashed line: no KCl in solution. Solution: 0.1 M HClO₄/5 mM Fe(ClO₄)₂/5 mM Fe(ClO₄)₃. Working electrode area: 4.2 mm². Reference: SCE. Counter: gold. Scan rate: 100 mV/s.

and depends on the presence of fixed charged groups in the polymer. Therefore, the retention of ionic phosphonic acid groups by PAPA-containing plasma polymers was of particular interest in this study. The ionic conductivity of the PAPA-containing plasma polymer films was demonstrated qualitatively by conductance measurements. These measurements showed that the relative conductivity of the plasma polymer membranes was increased by increasing the PAPA content of the comonomer feed. This result was supported by the FTIR evidence for intact phosphonic acid groups.

The ionic nature of PPPAPA was also demonstrated by observation of the Fe²⁺/Fe³⁺ oxidation kinetics at PPPAPA-coated gold using cyclic voltammetry. Figure 4 shows the cyclic voltammograms of a bare (uncoated) interdigitated gold electrode in aqueous 0.1 M HClO₄/5 mM Fe(ClO₄)₂/5 mM Fe(ClO₄)₃ solution, with and without 0.1 M KCl. This figure is instructive in explaining the voltammetry of the PPCTFE- and PPPAPA-coated gold electrodes (Figure 3). Bare gold in the presence of Cl⁻ (Figure 4, solid line) exhibits rapid Fe²⁺ oxidation kinetics,⁴⁴ as indicated by the large positive current peak near the formal redox potential for the Fe²⁺/Fe³⁺ couple (approximately 0.5 V vs SCE). In the absence of Cl⁻ (Figure 4, dashed line), the oxidation kinetics were slower, as evidenced by an oxidation peak current which was lower and shifted to higher potentials.

The initially depressed Fe²⁺ oxidation current exhibited by the PPPAPA-coated interdigitated electrode (Figure 3) was attributed to chloride ion exclusion by negatively charged phosphonic acid groups fixed within the PPPAPA films. Similar Cl⁻ exclusion has been observed with Nafion-coated gold electrodes in the presence of low levels of Cl⁻.⁴⁵ The increase in Fe²⁺ oxidation kinetics on subsequent sweeps, until an uncoated gold-like steady state was attained, was attributed to an increase in Cl⁻ concentration at the gold electrode surface. This occurred because the plasma polymer film was ineffective in excluding Cl⁻ as current was continuously passed through the electrode in the presence of the high Cl⁻ concentration (0.1 M KCl) in

the adjacent liquid electrolyte layer. The chloride penetration into the PPPAPA was reversible, since the sequence of voltammograms shown in Figure 3 were reproduced after rinsing the membrane with DD water.

The reproducibility of these data after rinsing indicated that the PPPAPA membrane was stable and well-adhered to the electrode. The adhesion of Nafion and its derivatives to smooth electrode surfaces in aqueous media has typically been poor.¹⁰ Similarly, strong adhesion of hydrophilic plasma polymers to inorganic substrates has been an elusive goal.^{20,46} The reproduction of the PPPAPA-coated gold voltammetry after rinsing, however, indicated the good adhesion of PPPAPA to the gold substrate in aqueous media.

Conclusions

This study has shown that adherent, ionically conductive membrane materials can be prepared by plasma copolymerization of CTFE and PAPA. The plasma-polymerized membranes possess covalently bound phosphonic acid groups and are highly cross-linked. Phosphonic acid content, cross-link density, and ionic conductivity increased with increasing PAPA in the comonomer feed. Retention of the phosphonic acid group by the plasma-polymerized membranes appeared to occur via cleavage of the C-C and C-P bonds in PAPA and subsequent reincorporation of the cleaved phosphonate fragment into the growing film. Cross-linking was the result of a high rate of fluorine ablation. The results of this study show that phosphonic acid content and cross-link density of the CTFE/PAPA plasma polymer membranes can be systematically increased by increasing the PAPA content in the comonomer feed. These results indicate that plasma copolymerization under fixed discharge conditions provides a novel and effective route to enhanced control over plasma polymer structure and composition.

Acknowledgment. The authors thank Robert C. Tucker for his assistance with the electrochemical characterization of the plasma polymers. This work was generously sponsored by the Edison Biotechnology Center and in part by the National Institutes of Health (Grant HL40047).

References and Notes

- (1) Current address: Redbank Research at Bellcore, Navesink Research and Engineering Laboratory, 331 Newman Springs Rd., Red Bank, NJ 07701.
- (2) Holliday, L., Ed. *Ionic Polymers*; Applied Science Publishers: London, 1975.
- (3) Dotson, R. L.; Woodard, K. E. *ACS Symp. Ser.* **1982**, *180*, 311.
- (4) Eisenberg, A.; Yeager, H. L., Eds. *Perfluorinated Ionomer Membranes*; ACS Symposium Series 180; American Chemical Society: Washington, DC, 1982.
- (5) McAuslan, B. R.; Johnson, G.; Hannan, G. N.; Norris, W. D.; Exner, T. J. *J. Biomed. Mater. Res.* **1988**, *22*, 963.
- (6) Grasel, T. G.; Cooper, S. L. *J. Biomed. Mater. Res.* **1989**, *23*, 311.
- (7) Okkema, A. Z.; Yu, X.-H.; Cooper, S. L. *Biomaterials* **1991**, *12*, 3.
- (8) Han, D. K.; Jeong, S. Y.; Kim, Y. H.; Min, B. G.; Cho, H. I. *J. Biomed. Mater. Res.* **1991**, *25*, 561.
- (9) Harrison, D. J.; Turner, R. F. B.; Baltes, H. P. *Anal. Chem.* **1988**, *60*, 2002.
- (10) Cha, C. S.; Chen, J.; Liu, P. F. *J. Electroanal. Chem.* **1993**, *345*, 463.
- (11) Kesting, R. A. *Synthetic Polymeric Membranes*; John Wiley and Sons: New York, 1985; Chapter 4.
- (12) Yeo, S. C.; Eisenberg, A. *J. Appl. Polym. Sci.* **1977**, *21*, 875.

- (13) Gierke, T. D.; Hsu, W. Y. *ACS Symp. Ser.* **1982**, *180*, 283.
- (14) Mauritz, K.; Hopfinger, A. J. In *Modern Aspects of Electrochemistry*; Bockris, J., Conway, B., White, R., Eds.; Plenum Press: New York, 1982; No. 14, Chapter 6.
- (15) Verbugge, M. W.; Hill, R. F. *J. Electrochem. Soc.* **1990**, *137*, 1131.
- (16) Ogumi, Z.; Uchimoto, Y.; Takehara, Z.-I. *J. Electrochem. Soc.* **1990**, *137*, 3319.
- (17) Yasuda, H. *Plasma Polymerization*; Academic Press, Inc.: Orlando, FL, 1985.
- (18) Burton, D. J. *Gov. Rep. Announce. Index (U.S.)* **1992**, *92*, 111.
- (19) Danilich, M. J. Ph.D. Thesis, Case Western Reserve University, Cleveland, OH, 1994.
- (20) Marchant, R. E.; Yu, D.; Khoo, C. *J. Polym. Sci., Polym. Chem.* **1989**, *27*, 881.
- (21) McCrackin, F. L. National Bureau of Standards Technical Note 479, 1969.
- (22) Johnson, S. D.; Anderson, J. M.; Marchant, J. M. *J. Biomed. Mater. Res.* **1992**, *26*, 915.
- (23) Wang, X. M.S. Thesis, Case Western Reserve University, Cleveland, OH, 1993.
- (24) Johnson, S. D. M.S. Thesis, Case Western Reserve University, 1993.
- (25) Adamson, A. W. *Physical Chemical of Surfaces*; 4th ed.; John Wiley and Sons: New York, 1982; Chapter 10.
- (26) Kaeble, D. H. *J. Adhes.* **1970**, *2*, 66.
- (27) Ratner, B. D.; McElroy, B. J. In *Spectroscopy in the Biomedical Sciences*; Gendreau, R. M., Ed.; CRC Press: Boca Raton, FL, 1986; Chapter 5.
- (28) Briggs, D. In *Electron Spectroscopy: Theory, Techniques and Application*; Brundle, C. R., Baker, A. D., Eds., Academic Press: New York, 1979; Vol. 3, Chapter 6.
- (29) Clark, D. T.; Feast, W. J.; Kilcast, D.; Musgrave, W. K. R. *J. Polym. Sci., Polym. Chem. Ed.* **1973**, *11*, 389.
- (30) Strobel, M.; Corn, S.; Lyons, C. S.; Korba, G. A. *J. Polym. Sci., Polym. Chem. Ed.* **1985**, *23*, 1125.
- (31) Inagaki, N.; Tasaka, S.; Park, M. S. *J. Appl. Polym. Sci.* **1990**, *40*, 143.
- (32) Bellamy, L. J. *The Infrared Spectra of Complex Molecules*; John Wiley and Sons, Inc.: New York, 1954.
- (33) O'Kane, D. F.; Rice, D. W. *J. Macromol. Sci., Chem.* **1976**, *A10*, 567.
- (34) Savage, C. R.; Timmons, R. B.; Lin, J. W. *Chem. Mater.* **1991**, *3*, 575.
- (35) Rao, C. N. R. *Chemical Applications of Infrared Spectroscopy*; Academic Press, Inc.: New York, 1963.
- (36) Brauholtz, J. T.; Hall, G. E.; Mann, F. G.; Sheppard, N. *J. Chem. Soc.* **1959**, 868.
- (37) Danilich, M. J.; Burton, D. J.; Marchant, R. E. *Vibr. Spectrosc.*, in press.
- (38) Zaretsky, M. C.; Mouyad, L.; Melcher, J. R. *IEEE Trans. Elect. Ins., EI-23* **1988**, *6*, 897.
- (39) Sanderson, R. T. *Chemical Bonds and Bond Energy*; Academic Press, Inc.: New York, 1971.
- (40) Chapman, B. *Glow Discharge Processes: Sputtering and Plasma Etching*; John Wiley and Sons, Inc.: New York, 1980.
- (41) Kay, E.; Dilks, A. *J. Vac. Sci. Technol.* **1981**, *18*, 1.
- (42) Iriyama, Y.; Yasuda, H. *J. Polym. Sci., Polym. Chem.* **1992**, *30*, 1731.
- (43) Yasuda, H.; Marsh, H. C.; Bumgarner, M. O.; Morosoff, N. *J. Appl. Polym. Sci.* **1975**, *19*, 2845.
- (44) Hung, N. C.; Nagy, Z. *J. Electrochem. Soc.* **1987**, *134*, 2215.
- (45) Chu, D.; Tryk, D.; Gervasio, D.; Yeager, E. *J. Electroanal. Chem.* **1989**, *272*, 277.
- (46) Marchant, R. E.; Johnson, S. D.; Schnieder, B. H.; Agger, M. P.; Anderson, J. M. *J. Biomed. Mater. Res.* **1990**, *4*, 1521.

MA9462520